Analysis of the Signal Transfer and Folding in N-Path Filters With a Series Inductance

Lammert Duipmans, Remko E. Struiksma, Eric A. M. Klumperink, *Senior Member, IEEE*, Bram Nauta, *Fellow, IEEE*, and Frank E. van Vliet, *Senior Member, IEEE*

***Abstract*—N-path filters exploiting switched-series-R-C networks can realize high-Q blocking-tolerant band-pass filters. Moreover, their center frequency is flexibly programmable by a digital clock. Unfortunately, the time variant nature of these circuits also results in unwanted signal folding. This paper proves analytically that folding can be reduced and band pass filtering can be improved by adding an inductance in series with the switched-R-C network. In contrast, a shunt capacitor degrades band-pass filter performance. The interaction between the reactive series impedance and the switched capacitors of an N-path filter complicates analysis due to memory effects associated with reactive components. Assuming N identical signal paths with $1/N$ duty cycle, we show it is possible to solve the set of differential equations, by assuming that the signals in each path only differ in delay. Analytical equations are verified versus simulations, and the benefits in filter properties and reduction in signal folding are demonstrated.**

***Index Terms*—Cognitive radio, commutated network filters, filter, frequency translated filtering, linear periodically time variant circuit, N-path filter, reconfigurable filter, software defined radio, switched capacitor filters, tunable filter.**

I. Introduction

TUNABLE filters with high linearity and strong blocker handling capability are highly wanted to realize reconfigurable radio receivers and enable cognitive radio [1]. Recent research has shown that N-path filters ($N \geq 3$) are promising candidates to realize tunable band-pass filters [2]–[12] and also simultaneous frequency and spatial domain filtering [13], [14]. Although the concept dates back to the 1960s [15], [16], only with the advent of nanometer CMOS technologies can such filters now operate at low GHz RF frequencies. Fig. 1 shows a 4-path filter with 4 capacitors and switches driven by multi-phase non-overlapping digital clocks that define the filter center frequency. Basically the input signal is mixed down, filtered, and mixed up again by the same set of switches, resulting in second order band-pass filter behavior, also without the inductor: essentially the low-pass R-C filter shape is shifted to around f_s. The associated bandwidth BW defined by the RC time and duty cycle of the clock can be as low as a few MHz, equal to a typical channel bandwidth. As GHz clock frequencies are possible, the $Q = f_s/BW$ can be high, e.g., a $Q > 100$ is feasible. Moreover, the linearity of passive mixers realized with MOS switches can be very good, and blockers in the order of 0 dBm can be handled provided the switches have sufficient overdrive voltage. As switches and capacitors scale well with CMOS downscaling, the technique can benefit from process scaling (see for instance [14] which compares a 65 nm and 28 nm chip).

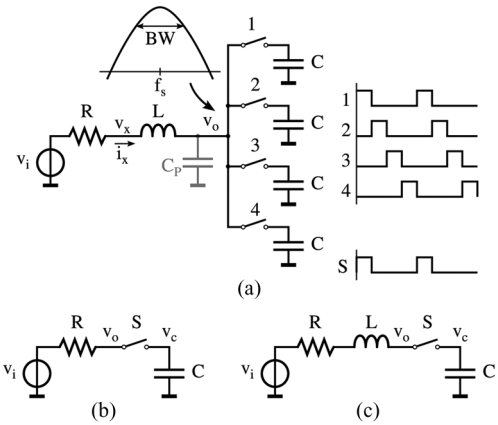

Fig. 1. (a) Single-ended 4-path switch-R-C filter with series inductor L and parasitic capacitance C_P. Switches are driven by non-overlapping clocks. Conditionally, the circuit can be split in independent single-ended "kernels," where: (b) is a switch-R-C kernel (index R); (c) is a switch-R-L-C kernel.

Unfortunately, the time variant nature of N-path filters due to the on/off switching also results in unwanted signal folding (somewhat similar to aliasing in samplers, but with attenuation due to the embedded low-pass filtering as we will see later). Hence, pre-filtering is wanted to attenuate signals that would otherwise fold on top of the wanted signal. Pre-filtering can also reduce harmonic passbands at multiples of the switching frequency, although these are less problematic than folding (they do not overlap with the main filter passband). Although using more paths allows for cancelling more harmonics and folding products [17], there is a limit to the number of feasible phases for a multi-phase clock because of process speed and power consumption. Moreover, phase errors limit the achievable cancellation of harmonic and folding responses. Hence, assistance by a pre-filter may be needed to achieve sufficient suppression of a problematic folding product. The strongest folding to the passband of interest occurs from $(N-1)f_s$, the folding sideband nearest to the passband [17]. For a 4-path this is around $f_{RF} \approx 3f_s$and for 8 paths around $f_{RF} \approx 7f_s$. As these frequencies are more than an octave away from the desired signal at $f_{RF} \approx f_s$, low-order low-pass pre-filtering can be enough to attenuate

Manuscript received June 11, 2014; revised July 26, 2014; accepted August 03, 2014. Date of publication October 14, 2014; date of current version January 06, 2015. This research was conducted as part of the Sensor Technology Applied in Reconfigurable systems for sustainable Security (STARS) project funded by the Dutch Government. This paper was recommended by Associate Editor P.-I. Mak.

L. Duipmans, R. E. Struiksma, E. A. M. Klumperink, and B. Nauta are with the University of Twente, Enschede 7500 AE, The Netherlands (e-mail: e.a.m.klumperink@utwente.nl).

F. E. van Vliet is with the University of Twente, Enschede 7500 AE, The Netherlands, and also with TNO, Den Haag 2509 JG, The Netherlands.

Color versions of one or more of the figures in this paper are available online at http://ieeexplore.ieee.org.

Digital Object Identifier 10.1109/TCSI.2014.2354772

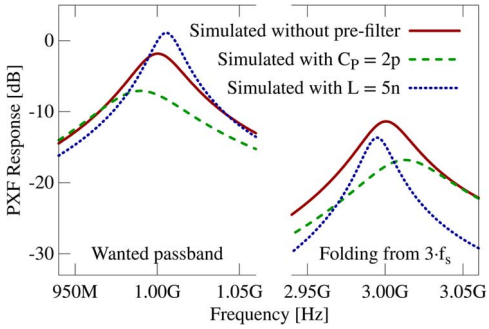

Fig. 2. Simulated periodic transfer function (PXF) for the wanted transfer and unwanted folding from $3f_s$ for the 4-path filter of Fig. 1(a), showing improvement with a series inductor $L(C_P = 0)$ and degradation with a shunt capacitor $C_P(L = 0)$, compared to the pre-filter less resistive case $(L = 0, C_P = 0)$.

folding products. However, filter design is less straightforward than one might expect. This is due to interaction between reactive pre-filter components with memory and the switched capacitors. The circuit in Fig. 1(a) with resistive source $(L = 0)$ can be analyzed by exploiting the lack of memory in a resistor, and the lack of interaction between the capacitor charges due to the non-overlapping clocks. Hence the circuit can be split in independent kernels (Fig. 1(b), [5], [18]), and the response of the complete system can be found by adding the responses of the kernels. However, if an inductor or capacitor is present between the signal source and switches, the states of the switched capacitors are also affected by the mutual interaction via this memory element. The purpose of this paper is to derive analytical equations describing this interaction and its impact on signal transfer and folding. Although it has been observed that adding a series inductor can improve the filter transfer and noise [19], [20], only approximate equations for the desired transfer function, the input impedance and noise are available [4], [21], [22], assuming the RF-frequency is $f_{RF} = f_s + \Delta f$, with $\Delta f \ll f_{LO}$. Broadband signal folding cannot be analyzed with these equations. This paper includes folding and extends the exact analysis in [5], [12], [18] to include memory effects for the case that a series inductance is added. We focus on this case as, in contrast to adding a shunt capacitor C_P before the switches, a series inductance increases passband gain and selectivity, while also reducing signal folding (see Fig. 2).

This paper is structured as follows: in Section II the analysis of the switched-series-R-C kernel in Fig. 1(b) is reviewed [5], [18]. This both serves as basis for the analysis of the case with series inductance [Fig. 1(c)] in Section III, and as benchmark to quantify filter improvements. Section IV compares analysis results with simulations and Section V presents conclusions.

II. N-Path Filter With Resistive Source Impedance

In [18] a detailed analysis of a switched series R-C network is presented that is also applicable to N-path filter analysis as shown in [5]. In this section, we quickly review the analysis for a resistive source impedance, as basis for the analysis with an inductive source impedance, which is done in the next section.

In a single-ended N-path filter the switches are driven by polyphase clocks, i.e., clocks with the same duty-cycle starting at regularly spaced intervals within the period time. The clocks do not overlap when high and the capacitor voltages are thus independent, which simplifies analysis. In Fig. 3, a timing diagram of the intervals in a general N-path filter is shown, where

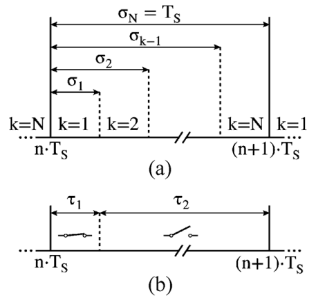

Fig. 3. Timing diagram for (a) the N-path filter, (b) the kernel to be analyzed, which contributes to $v_o(t)$ during $k = 1$.

σ_0 is defined to be 0. To simplify mathematical expressions, ideal switches will be assumed that switch infinitely fast between R_{off} of infinity and R_{on} of zero. Moreover, we assume that no time interval exists in which all switches are open, i.e., the clock duty-cycle is $1/N$, with N the number of paths. Thus only the switch in the k-th path will be closed during interval k, during an on-time T_s/N.

The analysis will now be performed by decomposing the N-path circuit in so-called "kernels" [18] as shown in Fig. 1(b). First, only one kernel will be analyzed. Other kernels have the same transfer function, except for a phase shift in the clock.

We can find the combined effect of all kernels in a polyphase system, using the analysis for one kernel and adding that phase shift term later, in subsection A. We choose the kernel for which the switch is closed during $k = 1$ for analysis, so τ_1 is the on-time of the switch and τ_2 the off-time, as shown in Fig. 3(b).

For zero switch resistance, the output voltage $v_o(t)$ is equal to one of the capacitor voltages. The kernel under analysis defines the output only during $k = 1$. Other kernels will provide the output during other intervals, each for exactly $1/N$th of T_s. This periodicity is crucial for the filter behavior and signal folding to be analyzed. In order to limit mathematical derivations, we will write equations in the same form as in [18], [23] and re-use the Fourier transform derived there [16]. To this end we will write differential equations as a function of t and k, where k relates to the time variant behavior. Considering the kernel in Fig. 1(b) during an interval identified by k, the following equation holds:

$$\frac{dv_c(t)}{dt} = A_{k,R}v_c(t) + C_{k,R}v_i(t), nT_s + \sigma_{k-1} \le t < nT_s + \sigma_k \tag{1}$$

We have a series-R-C network (index R) only during $k = 1$, so:

$$A_{1,R} = -\frac{1}{RC},\ C_{1,R} = \frac{1}{RC} \tag{2}$$

while the coefficients are 0 for other k values (the capacitor voltage doesn't change during the hold-phase). Following [16] we introduce a time windowed version $v_{c,k}(t)$ of the capacitor voltage, defined as:

$$v_{c,k}(t) = w_k(t) \cdot v_c(t) \tag{3}$$

$$w_k(t) = \begin{cases} 1, & nT_s + \sigma_{k-1} \le t < nT_s + \sigma_k \\ 0, & \text{elsewhere} \end{cases} \tag{4}$$

where $w_k(t)$ is a time windowing function that is useful from a mathematical point of view [16], and conveniently chosen so that the contributions of $v_{c,k}(t)$ to the output voltage $v_o(t)$ occur during this time window. The window can be modelled by step

functions and as derived in Appendix A, the differential equation for the kernel, valid for all t, can now be written as:

$$\frac{dv_{c,k}(t)}{dt} = A_{k,R}v_{c,k}(t) + C_{k,R}v_{i,k}(t) + \sum_{n=-\infty}^{\infty} v_c(t)\left(\delta(t-nT_s-\sigma_{k-1})-\delta(t-nT_s-\sigma_k)\right) \quad (5)$$

where the δ-functions add and subtract samples at interval ends, as discussed in [23, eq. (7)]. By applying the Fourier transqform to this equation, $V_{c,k}(f)$ is found [18, app. A]:

$$V_{c,k}(f) = \sum_{n=-\infty}^{\infty} H_{n,k,R}(f)V_i(f-nf_s) \quad (6)$$

where $H_{n,k,R}(f)$ is the transfer function associated with frequency shift nf_s, while index R refers to a purely resistive source ($L = 0$). Note that a frequency component $V_i(f)$ at the input not only contributes to $V_c(f)$ as in a Linear Time Invariant filter, *but also renders frequency shifted terms* ($V_i(f - nf_s)$). This renders signal folding to the pass band if an input signal exists at frequency spacing nf_s from the pass band, which should be minimized. Evaluating the Fourier transform gives [18]:

$$H_{n,k,R}(f) = \frac{1}{j2\pi f - A_{k,R}}\left(C_{k,R}\frac{1-e^{-j2\pi n/N}}{j2\pi n}e^{-j2\pi nf_s\sigma_{k-1}} + f_sG_{k-1,R}(f-nf_s)e^{-j2\pi nf_s\sigma_{k-1}} - f_sG_{k,R}(f-nf_s)e^{-j2\pi nf_s\sigma_k}\right) \quad (7)$$

Because the kernels are identical, it is sufficient to determine the transfer of only one of them. As we analyzed a kernel active during $k = 1$, i.e., $H_{n,1,R}(f)$. The functions $G_{0,R}$ and $G_{1,R}$ that are then required for (7) are [18, app. B]:

$$G_{0,R}(f) = \frac{1}{1+j2\pi fRC}\left(\frac{e^{j2\pi f\tau_1} - e^{\frac{-\tau_1}{RC}}}{e^{j2\pi fT_s} - e^{\frac{-\tau_1}{RC}}}\right) \quad (8)$$

$$G_{1,R}(f) = G_{0,R}(f)e^{j2\pi f\tau_2} \quad (9)$$

The function $G_{0,R}(f)$ is the transfer to the output voltage when sampled at nT_s (when the switch closes) and $G_{1,R}(f)$ when sampled at $nT_s + \sigma_1$ (when the switch opens). Because during τ_2 (when the switch is open) the voltage on the capacitor does not change, these transfers differ only by a delay.

A. Polyphase Multi-Kernel Combination

The final step is to combine the kernel transfer functions into one transfer function for the polyphase system. Assuming no switch resistance, kernel 1, active during $k = 1$, contributes to $V_o(f)$ via transfer function $H_{n,1,R}(f)$. The only difference between the kernels or paths in an N-path filter as depicted in Fig. 1 is the phase shift of the clocks driving the switches. With l defined as the path number and N the number of paths, the phase shift of the clock of kernel l compared to kernel 1 is $2\pi(l-1)/N$. The transfer function of the combined output then is equal to the following sum [18]:

$$H_{n,polyphase,R}(f) = \sum_{l=1}^{N} H_{n,1,R}(f)e^{\frac{j2\pi n(l-1)}{N}} = \begin{cases} 0, & n/N \neq \text{integer} \\ N \cdot H_{n,1,R}(f), & n/N = \text{integer} \end{cases} \quad (10)$$

with $H_{n,1,R}(f)$ the transfer of a single kernel calculated for the interval where the switch is on (note the periodicity with N). The output spectrum is given by:

$$V_o(f) = \sum_{n-=\infty}^{\infty} H_{n,polyphase,R}(f)V_i(f-nf_s) \quad (11)$$

It can be seen from (10) that $H_{n,polyphase,R}(f)$ is non-zero for $n = kN$, with k an integer. Hence, some of the harmonic folding terms remain un-cancelled, namely from input frequencies around $f_s - kNf_s$ to the desired filter band around f_s. (7) and (10) can be combined and simplified. The transfer function with $n = 0$ (no frequency shift) can be determined by taking the limit of the first term between brackets in (7) for n approaching zero. This leads to:

$$H_{0,polyphase,R}(f) = \frac{N}{j2\pi f + \frac{1}{RC}}\left(\frac{1}{NRC} + f_s \cdot (G_{0,R}(f) - G_{1,R}(f))\right) = H_R(f)\left(1 + \frac{1}{\Gamma^R}(G_{0,R}(f) - G_{1,R})\right) \quad (12)$$

Where:

$$H_R(f) = \frac{1}{1+j2\pi fRC} \quad (13)$$

$$\Gamma_R = \frac{T_s}{NRC} \quad (14)$$

Γ_R is the ratio between the switch-on time and the RC-time constant as introduced in [18], with the only difference that the duty-cycle is fixed here to $1/N$ to minimize signal loss [5]. For N-path filters, the $Q = 2\pi f_s/BW = 2\pi/\Gamma_R$, so for high Q we want $\Gamma_R \ll 2\pi$. Hence, we operate in the "slow" region [18], in which the RC time is much larger than the switch-on time (narrowband filtering, slow settling). Note that this is quite different from discrete-time switched-capacitor filters, where *fast* settling of capacitor voltages is required within one clock period.

The harmonic folding effects are characterized by (8) and (9) with n non-equal to zero. Taking into consideration that the on-time is always T_s/N and σ_0 is 0 we find:

$$H_{n,polyphase,R}(f) = \frac{H_R(f)}{\Gamma^R} \cdot (G_{0,R}(f-nf_s) - G_{1,R}(f-nf_s)), \quad n/N = \text{integer and } n \neq 0 \quad (15)$$

III. N-Path Filter With Inductive Source Impedance

In the current section, an N-path filter with a series inductance as shown in Fig. 1(a) is analyzed. The presence of such a "memory-element" results in interaction between the different paths. At the moment a switch closes, the inductor already carries a current which is dependent on the history of the voltage across the inductor, i.e., the previous path voltages.

The analysis starts again with decomposing the circuit into kernels [Fig. 1(c)]. However, now the differential equation valid during on-time τ_1 of the switch is of second order:

$$\frac{d^2v_c(t)}{dt^2} = A_k v_c(t) + B_k \frac{dv_c(t)}{dt} + C_k v_i(t), \quad nT_s + \sigma_{k-1} \le t < nT_s + \sigma_k \tag{16}$$

$$\text{With}: A_1 = -C_1 = \frac{-1}{LC}, \quad B_1 = -\frac{R}{L} \tag{17}$$

while the coefficients are zero for other values of k. The voltage transfer function can be found by applying the Fourier transform on the differential equation above. In order to make this possible, the equation has to be made valid for all t. This process is described in Appendix A and results in:

$$\begin{aligned}\frac{d^2v_{c,k}(t)}{dt^2} &= A_k v_{c,k}(t) + B_k \frac{dv_{c,k}(t)}{dt} + C_k v_{i,k}(t) \\ &+ \sum_{n=-\infty}^{\infty} \Big\{ -B_k v_c(t) \left(\delta(t - nT_s - \sigma_{k-1}) - \delta(t - nT_s - \sigma_k)\right) \\ &+ \frac{d\left(v_c(t)\left(\delta(t - nT_s - \sigma_{k-1}) - \delta(t - nT_s - \sigma_k)\right)\right)}{dt} \\ &+ \frac{dv_c(t)}{dt}\left(\delta(t - nT_s - \sigma_{k-1}) - \delta(t - nT_s - \sigma_k)\right) \Big\}\end{aligned} \tag{18}$$

For evaluating the above equation, the sampled output voltage terms at the switching moments are needed and also the derivative of the output voltage at those moments. In the next section, the process of how to express these terms as a function of the input voltage will be described. When these terms are known, the Fourier transform can be performed on (18) leading to the wanted transfer function.

For sinusoidal input voltage $e^{j2\pi ft}$ the general solution to (16) is of the form [24]:

$$v_c(t) = c_1 e^{s_1(t-t_0)} + c_2 e^{s_2(t-t_0)} + c_3 e^{j2\pi f(t-t_0)} \tag{19}$$

in which the first two terms are the solution of the homogeneous equation, with s_1 and s_2 the roots of the characteristic polynomial [24, Lesson 20]:

$$s_{1,2} = \frac{B_k}{2} \pm \sqrt{\left(\frac{B_k}{2}\right)^2 + A_k} = \frac{R}{2L} \pm \sqrt{\left(\frac{R}{2L}\right)^2 - \frac{1}{LC}} \tag{20}$$

The constants will be solved from the initial conditions. The last term in (19) represents the particular solution [24, lesson 21]. Substitution of this solution in (16) and evaluation for $t = t_0$ leads to:

$$\begin{aligned}c_3 &= e^{j2\pi ft_0} \frac{C_k}{-A_k - j2\pi f B_k - (2\pi f)^2} \\ &= e^{j2\pi ft_0} \cdot H(f)\end{aligned} \tag{21}$$

For $k = 1$:

$$H(f) = \frac{1}{1 + j2\pi fRC - (2\pi f)^2 LC} \tag{22}$$

The function $H(f)$ is equal to the frequency domain transfer function $V_c(f)/V_i(f)$ of a single kernel with the switch closed.

The expression of the output voltage during the on-time of the switch is dependent on the initial conditions, i.e., the output voltage at the time instant the particular switch closes and its derivative (or strictly speaking the related current through the inductor). Suppose, the time instant of the closing of the switch is t_0. The remaining constants can now be determined by solving the following two equations for c_1 and c_2:

$$v_c(t_0) = c_1 + c_2 + c_3 \tag{23}$$

$$v_c'(t_0) = c_1 s_1 + c_2 s_2 + c_3 j2\pi f \tag{24}$$

Resulting in:

$$c_1 = v_c(t_0)\frac{s_2}{s_2 - s_1} - v_c'(t_0)\frac{1}{s_2 - s_1} + c_3\frac{j2\pi f - s_2}{s_2 - s_1} \tag{25}$$

$$c_2 = v_c(t_0)\frac{-s_1}{s_2 - s_1} + v_c'(t_0)\frac{1}{s_2 - s_1} + c_3\frac{s_1 - j2\pi f}{s_2 - s_1} \tag{26}$$

Substitution of the constants in (19) gives:

$$\begin{aligned}v_c(t) = v_c(t_0)&\frac{s_2 e^{s_1(t-t_0)} - s_1 e^{s_2(t-t_0)}}{s_2 - s_1} \\ &+ v_c'(t_0)\frac{e^{s_2(t-t_0)} - e^{s_1(t-t_0)}}{s_2 - s_1} \\ &+ e^{j2\pi ft_0} H(f)\left(e^{j2\pi f(t-t_0)} - e^{s_1(t-t_0)} \right. \\ &\left. + \frac{e^{s_2(t-t_0)} - e^{s_1(t-t_0)}}{s_2 - s_1}(s_1 - j2\pi f)\right)\end{aligned} \tag{27}$$

And for the derivative of the output voltage:

$$\begin{aligned}v_c'(t) = v_c(t_0)&\frac{s_1 s_2 e^{s_1(t-t_0)} - s_1 s_2 e^{s_2(t-t_0)}}{s_2 - s_1} \\ &+ v_c'(t_0)\frac{s_2 e^{s_2(t-t_0)} - s_1 e^{s_1(t-t_0)}}{s_2 - s_1} \\ &+ e^{j2\pi ft_0} H(f)\left(j2\pi f e^{j2\pi f(t-t_0)} - s_1 e^{s_1(t-t_0)} \right. \\ &\left. + \frac{s_2 e^{s_2(t-t_0)} - s_1 e^{s_1(t-t_0)}}{s_2 - s_1}(s_1 - j2\pi f)\right)\end{aligned} \tag{28}$$

Using these equations, the output voltage and the derivative of the output voltage at the end of the on-time of the switch can be calculated, given the initial conditions. Setting the time instant of closing of the switch at $t = nT_s$ and assuming that the on-time of the switch is equal to τ_1 (see Fig. 3), the following equations can be composed:

$$v_c(nT_s + \sigma_1) = \alpha \cdot v_c(nT_s) + \beta \cdot v_c'(nT_s) + \gamma(f) \cdot e^{j2\pi fnT_s} \tag{29}$$

$$v_c'(nT_s + \sigma_1) = \alpha' \cdot v_c(nT_s) + \beta' \cdot v_c'(nT_s) + \gamma'(f) \cdot e^{j2\pi fnT_s} \tag{30}$$

$$\alpha = \frac{s_2 e^{s_1\tau_1} - s_1 e^{s_2\tau_1}}{s_2 - s_1} \tag{31}$$

$$\beta = \frac{e^{s_2\tau_1} - e^{s_1\tau_1}}{s_2 - s_1} \tag{32}$$

$$\alpha' = \frac{s_1 s_2 e^{s_1\tau_1} - s_1 s_2 e^{s_2\tau_1}}{s_2 - s_1} \tag{33}$$

$$\beta' = \frac{s_2 e^{s_2\tau_1} - s_1 e^{s_1\tau_1}}{s_2 - s_1} \tag{34}$$

$$\gamma(f) = H(f)\left(e^{j2\pi f\tau_1} - e^{s_1\tau_1} + \beta\cdot(s_1 + j2\pi f)\right) \quad (35)$$

$$\gamma'(f) = H(f)\left(j2\pi f e^{j2\pi f\tau_1} - s_1 e^{s_1\tau_1} + \beta'(s_1 + j2\pi f)\right) \quad (36)$$

From now on, the process comes down to setting up the difference equations for the sampled v_c and v_c'. Since the capacitor voltage remains constant during the interval the switch is off, we also write:

$$v_c\left((n+1)T_s\right) = \alpha \cdot v_c(nT_s) + \beta \cdot v_c'(nT_s) + \gamma(f)e^{j2\pi f nT_s} \quad (37)$$

For composing the difference equation for v_c', *it is assumed that the current through the inductor at the moment the switch opens is equal to the current at the moment the switch of the next path closes*. As a consequence, assuming equal capacitors, this equality also holds for the derivative of the output voltage at these time instants. With a duty-cycle of exactly $1/N$, this assumption will indeed be valid. Using this result:

$$\begin{aligned} v_{c,l}'\left((n+1)T_s\right) = {} & \alpha' \cdot v_{c,l-1}'\left((n+1)T_s - \frac{T_s}{N}\right) \\ & + \beta' \cdot v_{c,l-1}'\left((n+1)T_s - \frac{T_s}{N}\right) \\ & + \gamma'(f) \cdot e^{j2\pi f}\left((n+1)T_s - \frac{T_s}{N}\right) \end{aligned} \quad (38)$$

In which $v_{c,l}$ is the capacitor voltage of path number l. At first sight, this difference equation seems difficult to solve, because it is dependent on the output state of the previous path, which is again dependent on the output state of the path before that, and so on. However, all paths are identical, albeit that the time interval in which they are connected to the output differs. As these intervals are spaced apart by T_s/N, *different paths will see a phase shifted version of the input signal.* Assuming an input voltage $v_i = e^{j2\pi ft}$, a relation between different path voltages of the following form should be expected:

$$v_{c,l-1}\left((n+1)T_s - \frac{T_s}{N}\right) = v_{c,l}\left((n+1)T_s\right)e^{-\frac{j2\pi fT_s}{N}} \quad (39)$$

A similar relation also holds for v_c':

$$v_{c,l-1}'\left((n+1)T_s - \frac{T_s}{N}\right) = v_{c,l}'\left((n+1)T_s\right)e^{-\frac{j2\pi fT_s}{N}} \quad (40)$$

With help of the last two equations we can write (38) as:

$$\begin{aligned} v_c'\left((n+1)T_s\right) = {} & \alpha' \cdot e^{-\frac{j2\pi fT_s}{N}} v_c\left((n+1)T_s\right)\beta' \\ & \cdot e^{-\frac{j2\pi fT_s}{N}} v_c'\left((n+1)T_s\right) + \gamma'(f)\cdot e^{j2\pi f\left((n+1)T_s - \frac{T_s}{N}\right)} \end{aligned} \quad (41)$$

where the subscript l is left out, because the function is no longer dependent on the path number. The next step is to solve for $v_c'((n+1)T_s)$ and substituting $(n-1)$ for n leading to:

$$v_c'(nT_s) = \frac{\alpha'}{e^{\frac{j2\pi fT_s}{N}} - \beta'} v_c(nT_s) + \frac{\gamma'(f)}{e^{\frac{j2\pi fT_s}{N}} - \beta'} e^{j2\pi f nT_s} \quad (42)$$

Substituting this into (37) we get:

$$\begin{aligned} v_c\left((n+1)T_s\right) = {} & \left(\alpha + \frac{\alpha'\beta}{e^{\frac{j2\pi fT_s}{N}} - \beta'}\right) v_c(nT_s) \\ & + \left(\gamma(f) + \frac{\gamma'(f)\cdot\beta}{e^{\frac{j2\pi fT_s}{N}} - \beta'}\right) e^{j2\pi f nT_s} \end{aligned} \quad (43)$$

This equation is of the same form as [18, eq. 87] and leads to the following steady state solution:

$$v_c(nT_s) = G_0(f)\cdot e^{j2\pi f nT_s} \quad (44)$$

With:

$$G_0(f) = \frac{\gamma(f) + \frac{\gamma'(f)\cdot\beta}{e^{\frac{j2\pi fT_s}{N}} - \beta'}}{e^{j2\pi fT_s} - \left(\alpha + \frac{\alpha'\beta}{e^{\frac{j2\pi fT_s}{N}} - \beta'}\right)} \quad (45)$$

Using (44), $v_c'(nT_s)$ can be determined using (42):

$$v_c'(nT_s) = I_0(f)\cdot e^{j2\pi f nT_s} \quad (46)$$

With:

$$I_0(f) = \frac{\alpha'}{e^{\frac{j2\pi fT_s}{N}} - \beta'} G_0(f) + \frac{\gamma'(f)}{e^{\frac{j2\pi fT_s}{N}} - \beta'} \quad (47)$$

Next, the goal is to find G_1 and I_1 (or equivalently: $v_c(nT_s + \sigma_1)$ and $v_c'(nT_s + \sigma_1)$):

$$\begin{aligned} v_c(nT_s + \sigma_1) &= \alpha \cdot v_c(nT_s) + \beta \cdot v_c'(nT_s) + \gamma(f)\cdot e^{j2\pi f nT_s} \\ &= \left(\alpha \cdot G_0(f) + \beta \cdot I_0(f) + \gamma(f)\right) e^{j2\pi f nT_s} \end{aligned} \quad (48)$$

Hence:

$$G_1(f) = \left(\alpha \cdot G_0(f) + \beta \cdot I_0(f) + \gamma(f)\right)\cdot e^{\frac{j2\pi fT_s}{N}} \quad (49)$$

When using (45) and (47) to evaluate (49), after some straightforward mathematics we get:

$$G_1(f) = G_0(f)e^{j2\pi f\left(T_s - \frac{T_s}{N}\right)} \quad (50)$$

Note that this relation was also found for the case without a reactive component. The procedure for finding I_1 is similar:

$$\begin{aligned} v_c'(nT_s + \sigma_1) &= \alpha' \cdot v_c(nT_s) + \beta' \cdot v_c'(nT_s) + \gamma'(f)\cdot e^{j2\pi f nT_s} \\ &= \left(\alpha' \cdot G_0(f) + \beta' \cdot I_0(f) + \gamma'(f)\right) e^{j2\pi f nT_s} \quad (51) \\ I_1(f) &= \left(\alpha' \cdot G_0(f) + \beta' \cdot I_0(f) + \gamma'(f)\right)\cdot e^{-\frac{j2\pi fT_s}{N}} \quad (52) \end{aligned}$$

After expressing G_0 in terms of I_0 by means of (47) and substitution in (52), the following simple result arises:

$$I_1(f) = I_0(f) \quad (53)$$

Using the functions $G(f)$ and $I(f)$, the Fourier transform can now be applied to (18) following a similar approach as [18, app. A and B]. However, not only the Fourier transform of the

capacitor voltage [18, eq. 77], but also that of the derivative of the capacitor voltage is needed, for which we find:

$$\sum_{n=-\infty}^{\infty} \mathcal{F}\left(\frac{dv_c(t)}{dt}\delta(t-nT_s-\sigma_k)\right) = \sum_{n=-\infty}^{\infty} I_k(f-nf_s)f_s e^{-\frac{j2\pi n}{N}} V_i(f-nf_s) \quad (54)$$

We can then find the solution for one kernel. As all kernels are equal, their response is equal apart from a phase shift and hence calculating only $H_{n,1}$ is sufficient. In (10) we see that the polyphase transfer function will only produce results non-equal to zero when n/N is an integer. Considering that $\sigma_0 = 0$ and $\sigma_1 = \tau_1 = T_s/N = 1/(Nf_s)$, after some math we get:

$$\begin{aligned} &H_{n,1}(f) \\ &= \frac{1}{-(2\pi f)^2 - j2\pi f B_1 - A_1} \\ &\times \left(C_1 \frac{1-e^{-j2\pi n f_s \tau_1}}{j2\pi n}\right. \\ &\quad +(-B_1 + j2\pi f)\left(f_s G_0(f-nf_s) - f_s G_1(f-nf_s)\right) \\ &\quad \left. + f_s I_0(f-nf_s) - f_s I_1(f-nf_s)\right), \quad \frac{n}{N} = \text{integer} \end{aligned} \quad (55)$$

By using (10), filling in the correct coefficients as defined in (17) and taking into account that I_1 is equal to I_0, the polyphase transfer can be determined:

$$\begin{aligned} &H_{n,polyphase}(f) \\ &= H(f)\cdot N\left(\frac{1-e^{-j2\pi n f_s \tau_1}}{j2\pi n}\right. \\ &\quad +(RC+j2\pi fLC)\cdot f_s\left(G_0(f-nf_s)\right. \\ &\quad \left.\left. -G_1(f-nf_s)\right)\right), \quad \frac{n}{N} = \text{integer} \end{aligned} \quad (56)$$

$$= \begin{cases} 0, & \frac{n}{N} \neq \text{integer} \end{cases} \quad (57)$$

IV. Model Verification and Application

To verify the analysis, the transfer function was calculated and simulated for a 4-path filter with the default parameters given in Table I: f_s of 1 GHz, R of 50 Ω, C of 50 pF and an inductance of 0 and 10 nH. Fig. 4 shows the simulated and calculated curves are identical, confirming correct analysis. We will now compare some results for the resistive and inductive source impedance and show that adding an inductor can improve filter properties significantly. First the filter shape will be discussed in Section IV-A, then the input impedance (Section IV-B), noise (Section IV-C), harmonic response (Section IV-D), and finally the unwanted signal folding (Section IV-E).

A. Filter Shape

Substituting $n = 0$ in (56) and taking the limit of the first term between brackets for n approaching zero, yields:

$$\begin{aligned} &H_{0,polyphase}(f) \\ &= N\cdot H(f)\cdot\left(\frac{1}{N} + (RC+j2\pi fLC)\left(f_s G_0(f) - f_s G_1(f)\right)\right) \\ &= H(f)\left(1+\frac{1}{\Gamma(f)}\left(G_0(f)-G_1(f)\right)\right) \end{aligned} \quad (58)$$

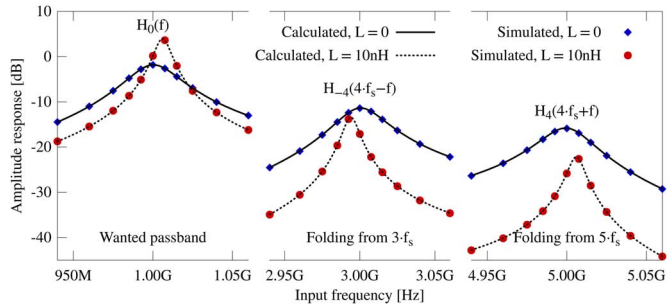

Fig. 4. Calculated and simulated $H_0(f)$, $H_{-4}(f)$ and $H_4(f)$, showing increased passband gain and reduced folding to the pass-band with inductor.

TABLE I
Default Values Used for Simulations

Symbol	Quantity	Value
f_s	Switching frequency	1 GHz
R	Filter Resistance	50 Ω
C	Filter Capacitance	50 pF
L	Series inductance	10nH or variable as indicated

with:

$$H(f) = \frac{1}{1+j2\pi fRC-(2\pi f)^2 LC} \quad (59)$$

$$\Gamma(f) = \frac{\frac{T_s}{N}}{RC+j2\pi fLC} = \frac{j2\pi fT_s}{N}\cdot\frac{H(f)}{1-H(f)} \quad (60)$$

This equation is of the same form as (12), but $H(f)$ is a second order low-pass function instead of a first order function and Γ is now also a function of frequency f due to the extra LC-term in the denominator Actually, (58) reduces to a regular second order low-pass function when Γ approaches infinity. However, this occurs when T_s goes to infinity, i.e., when the switching is eliminated and only one switch is permanently on. Hence, the first term between brackets represents low-pass behavior. The second term in (58) with G_0 and G_1 contains exponentials rendering repetitive peaks in the transfer characteristic at multiples of the switching frequency. To understand this intuitively, please refer to the time domain analysis in [5]. When Γ decreases, these peaks become narrower, i.e., quality factor increases. Compared to a resistive source impedance, there is an additional LC-term in the denominator of Γ, so that the series inductance renders an extra degree of freedom to adjust the filter. If the bandwidth of this filter is compared to that of a filter with resistive source impedance, it appears that the same bandwidth can be realized with a lower capacitance.

B. Input Impedance

We define an input impedance close to the fundamental as [5]:

$$Z_{x,0} = \frac{v_{x,0}(f)}{i_{x,0}(f)} = \frac{H_0(f)R + j2\pi fL}{1-H_0(f)} \quad (61)$$

Fig. 5 shows a plot of this impedance for two L-values. As $H_0(f)$ contains imaginary terms due to the up-converted impedance of the baseband capacitors, there is a dip in

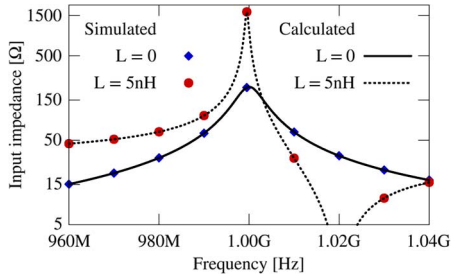

Fig. 5. Input impedance versus RF-frequency for $f_s = 1$ GHz.

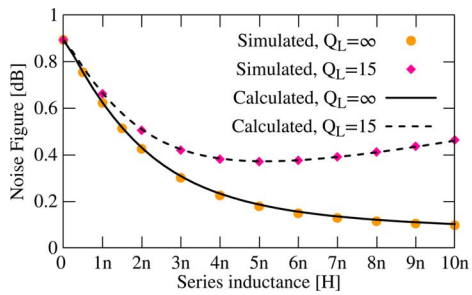

Fig. 6. Improvement in Noise Figure due to reduced noise folding.

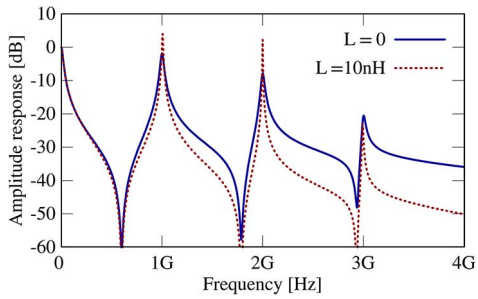

Fig. 7. Amplitude of $H_0(f)$ for a 4-path filter, using the values in Table I.

impedance for $L = 5\text{nH}$, because the R- and L-term in the numerator of (61) largely cancel each other at 1.02 GHz.

C. Noise Figure

The noise figure can be written as the total output noise divided by the output noise contribution from the source via the intended frequency translation:

$$F = \frac{\sum_{n=-\infty}^{\infty} H_n(f)^2}{H_0(f)^2} \tag{62}$$

Fig. 6 shows that adding a series inductor improves the noise figure, as expected, due to the reduced noise folding. In practice finite inductor-Q will limit the improvement as is also shown.

D. Harmonic Responses

As can be seen in Fig. 7, the N-path filter also has harmonic responses at mf_s.

Using (58) the filter response near harmonics of the switching frequency was analyzed versus inductance value. In Fig. 8, the absolute value of the peaks at a multiple m of the switching frequency is represented as a function of the series inductance. The values are calculated for a 4-path filter with f_s of 1 GHz, C of 50 pF and R of 50 Ω. It is apparent from the graph that the gain in the pass band for $m = 1$, i.e., the value of the peak

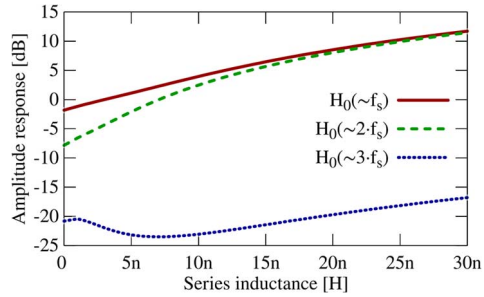

Fig. 8. Calculated peak values of the transfer function near the fundamental and second and third harmonic.

at f_s, is a strongly increasing function of L and can be much bigger than 1. Note that this concerns voltage, not power gain. The second harmonic response even grows faster with inductance, but can be cancelled in a fully differential topology. The third harmonic suppression compared to the fundamental benefits from increasing inductance especially for 1–10 nH.

E. Effect of Folding (Aliasing)

Next, the unwanted signal folding effects will be treated. The transfer of the N-path filter with n unequal to zero is given by:

$$H_{n,polyphase}(f) = H(f) \cdot \frac{1}{\Gamma(f)} \left(G_0(f - nf_s) - G_1(f - nf_s)\right) \tag{63}$$

If G_0 is evaluated for a frequency shifted input using (45), it appears that the only term dependent on nf_s is $H(f)$. For the remaining terms, the n dependency reduces to a phase shift of 2π in the argument of the exponents. Using this result, the following relation can be written:

$$G_0(f - nf_s) = G_0 \cdot \frac{H(f - nf_s)}{H(f)} \tag{64}$$

If we also do this for G_1 and substitute in (63), we can calculate the ratio of a folded term to the wanted term, and using (58) we get:

$$\frac{H_n(f)}{H_0(f)} = \frac{H(f - nf_s)}{H(f)} \cdot \frac{1}{1 + \frac{\Gamma(f)}{G_0(f) - G_1(f)}}, \quad \frac{n}{N} = \text{integer and } n \neq 0 \tag{65}$$

If $G_0 - G_1$ is sufficiently high and Γ is small, the last term in (65) reduces to a value close to one. This assumption is true for N-path filters with a gain close to or above 1 at frequency f_s. The following approximation holds then:

$$\frac{H_n(f_s)}{H_0(f_s)} \approx \frac{H(f_s - nf_s)}{H(f_s)}, \quad \frac{n}{N} = \text{integer} \tag{66}$$

This is a very interesting outcome: it appears that the signal folding to f_s is suppressed by low-pass filter $H(f)$. In other words, the *suppression of the folded components will only be dependent on the low-pass network (with transfer function H(f)) that the input sees when the switch is closed* (see Fig. 9). This is also the case for an N-path filter with resistive source impedance, because (12) and (15) are equivalent to (58) and (63). The only difference is that the function $H(f)$ is now a second order low-pass function instead of a first order function.

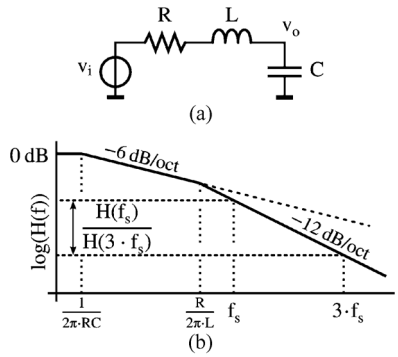

Fig. 9. (a) Low-pass filter obtained by closing the switch of the kernel. (b) The resulting transfer function with the relevant rejection ratio.

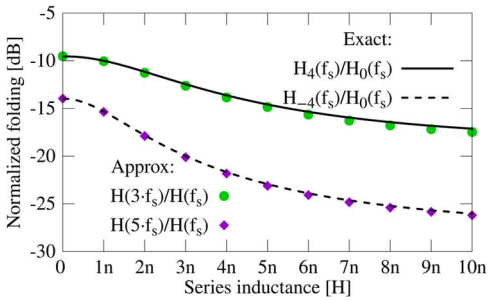

Fig. 10. Calculated folding for $f_s = 1$ GHz and variable L, both equation (65) (lines) and approximation equation (66) (dots), showing reduction for increasing inductance.

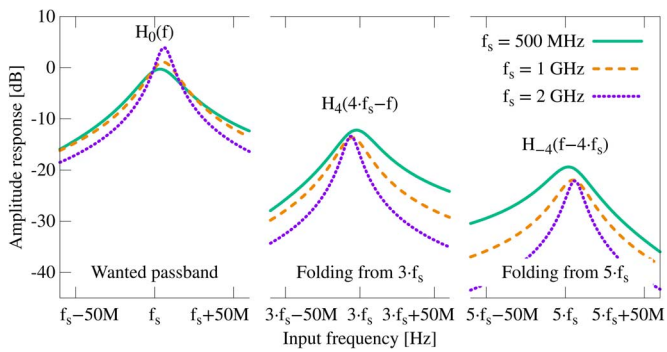

Fig. 11. Calculated wanted passband and unwanted folding for a fixed series inductance of 5 nH and f_s equal to 0.5, 1 and 2 GHz.

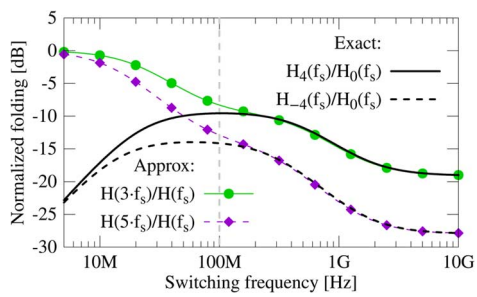

Fig. 12. Calculated folding [exact and approximate (lines with markers)] with $L = 5$ nH, showing good approximation for $f_s > 1/N \cdot R \cdot C (= 100$ MHz).

This means that the suppression of components folding back to the desired band can be much higher. To quantify this effect, let's assume that both f_s and $f_s - nf_s$ will fall outside the passband on the -12 dB/octave slope of the low-pass function. Now, the ratio in (66) can be approximated by:

$$\frac{H_n(f_s)}{H_0(f_s)} \approx \left(\frac{f_s}{f_s - nf_s}\right)^2, \qquad \frac{n}{N} = integer \tag{67}$$

The nearest component that folds back to the band of interest in a 4-path filter is the input shifted by $4f_s (n = 4)$. Hence an RF signal at $3f_s$ or $5f_s$ is shifted to f_s and falls on top of the filter band. As $3f_s$ is closer to f_s and hence more problematic, Fig. 9(b) graphically shows the relevant "pre-filter"[1] function H(f), which should now be evaluated at f_s and $3f_s$. Ratio $H(3f_s)/H(f_s)$ gives the attenuation for the folding compared to the wanted signal at $f_{RF} = f_s$ (see Fig. 9(b), a rough estimate is $(1/3)^2$). Fig. 10 plots the calculated folding versus L-value, both for the exact and approximate (66). Clearly, more folding reduction is usually wanted and one might wonder what happens for more paths. For an 8-path filter, the folding from $7f_s$ is suppressed to roughly $(1/7)^2$ or -34 dB (versus -17 dB for $L = 0$). Still often, more attenuation is desired and extra low-pass pre-filtering should be added. From the equations derived in the previous section, it appears that the function $G_0(f)$ is linearly related to the low-pass function $H(f)$, both for a first order filter (resistive source impedance) and a second order filter (inductive source impedance). This $H(f)$ dependency results from the particular solution of the differential equation. For a higher order pre-filter, a higher order transfer function and more filtering will likely result, but demonstrating this is left as future work.

The folding from $3f_s$ reduces from about -9 to -17 dB when L increases from 0 to 10 nH. In practice a fixed value of L will often be used, and then it may be interesting to see how the passband shape varies and how folding reduction varies as a function of the target center frequency f_s. The results are shown in Fig. 11. It can be verified that the best passband gain and least (relative) folding from $3f_s$ occurs at 2 GHz.

It should be noted that the results above assume an ideal inductor. A practical inductor may show parasitic capacitance to ground, which may have detrimental effects. Further research is needed to quantify what is feasible in practice, where this paper derives the ideal limit. The model in Fig. 9 with the "pre-filter" concept is intuitively attractive. However, it should be noted that it is an approximation which is only valid if $f_s \cdot N \cdot R \cdot C > 1$. Fig. 12 illustrates model validity limits for $L = 5$ nH, showing a good match above 100 MHz.

V. Conclusions

Analytical equations for the transfer function and signal folding of single-ended N-path filters with resistive and inductive series impedance have been derived. The analysis assumes ideal switches that switch instantly from an on-resistance of zero to an off-resistance of infinity. Furthermore, the duty-cycle is assumed ideal, i.e., equal to $1/N$.

The resulting equations have been examined and show that the addition of a series inductance results in improved band pass filter behavior. Increasing this inductance increases the in-band voltage gain and reduces the bandwidth, while also reducing noise and odd order harmonic responses. Moreover, and even more important for realizing a practical N-path filter, the addition of an inductor increases the suppression of signal folding from $(N-1)f_s$ to f_s. Interestingly, a good estimate for the filtering of folding products can be obtained by simply considering

[1]Strictly speaking this filter is not a separate pre-filter but an intrinsic part of the time variant circuit. Still, given our aim to reduce folding and given the filter transfer is multiplied with the N-path transfer function, we use this term.

the low-pass filter that results when only one switch of the filter is continuously closed.

APPENDIX

When looking at a single R-C kernel, during the on-time of the switch, the system is linear time invariant and the voltage is described by differential (1). Using step function $u(t)$, this equation can be adapted to one valid for all t as follows:

$$\begin{aligned}\frac{dv_c(t)}{dt}&\sum_{n=-\infty}^{\infty}\left(u(t-nT_s-\sigma_{k-1})-u(t-nT_s-\sigma_k)\right)\\&=\left(A_{k,R}v_c(t)+C_{k,R}v_i(t)\right)\\&\cdot\sum_{n=-\infty}^{\infty}\left(u(t-nT_s-\sigma_{k-1})-u(t-nT_s-\sigma_k)\right)\end{aligned}\quad(68)$$

This equation also defines v_c during interval k, i.e., $v_{c,k}$. Since $v_{c,k}$ is equal to v_c within interval k and zero outside this interval, $v_{c,k}$ can be written as:

$$v_{c,k}(t)=v_c(t)\sum_{n=-\infty}^{\infty}\left(u(t-nT_s-\sigma_{k-1})-u(t-nT_s-\sigma_k)\right)\quad(69)$$

For simplicity, during further calculations for one kernel the summation is left out in this expression and $n=0$ is substituted. In the end, the summation and time shift nT_s will be reintroduced when combining to a polyphase system. Hence, the simplified $v_{c,k}$ will be:

$$v_{c,k}(t)=v_c(t)\left(u(t-\sigma_{k-1})-u(t-\sigma_k)\right)\quad(70)$$

The same can be done for $v_{i,k}$ by simply replacing v_c by v_i in the above equation. Using the product rule, the derivative of $v_{c,k}$ can be calculated as well:

$$\begin{aligned}\frac{dv_{c,k}(t)}{dt}=&\frac{dv_c(t)}{dt}\left(u(t-\sigma_{k-1})-u(t-\sigma_k)\right)\\&+v_c(t)\left(\delta(t-\sigma_{k-1})-\delta(t-\sigma_k)\right)\end{aligned}\quad(71)$$

Applying the same simplifications to (68) yields:

$$\begin{aligned}&\frac{dv_c(t)}{dt}\left(u(t-\sigma_{k-1})-u(t-\sigma_k)\right)\\&=\left(A_{k,R}v_c(t)+C_{k,R}v_i(t)\right)\left(u(t-\sigma_{k-1})-u(t-\sigma_k)\right)\end{aligned}\quad(72)$$

Using (70) and (71), (72) can easily be expressed in terms of $v_{c,k}$ and $v_{i,k}$:

$$\begin{aligned}\frac{dv_{c,k}(t)}{dt}&-v_c(t)\left(\delta(t-\sigma_{k-1})-\delta(t-\sigma_k)\right)\\&=A_{k,R}v_{c,k}(t)+C_{k,R}v_{i,k}(t)\end{aligned}\quad(73)$$

When the Dirac delta functions between brackets are replaced by the infinite sum of Dirac functions and time shift nT_s is reintroduced, the result is (5).

For the R-L-C case, the equation that is valid for all t, equivalent to (72), is as follows:

$$\begin{aligned}&\frac{d^2v_c(t)}{dt^2}\left(u(t-\sigma_{k-1})-u(t-\sigma_k)\right)=\left(A_kv_c(t)\right.\\&\left.+B_k\frac{dv_c(t)}{dt}+C_kv_i(t)\right)\cdot\left(u(t-\sigma_{k-1})-u(t-\sigma_k)\right)\end{aligned}\quad(74)$$

As for the first order differential equation, the above equation should be expressed in terms of $v_{c,k}$. For this case, a second derivative of $v_{c,k}$ is also needed:

$$\begin{aligned}\frac{d^2v_{c,k}(t)}{dt^2}=&\frac{d^2v_c(t)}{dt^2}\left(u(t-\sigma_{k-1})-u(t-\sigma_k)\right)\\&+\frac{dv_c(t)}{dt}\left(\delta(t-\sigma_{k-1})-\delta(t-\sigma_k)\right)\\&+\frac{d\left((v_c(t)(\delta(t-\sigma_{k-1})-\delta(t-\sigma_k))\right)}{dt}\end{aligned}\quad(75)$$

Then, using (70), (71) and (75), (74) can be rewritten as:

$$\begin{aligned}&\frac{d^2v_{c,k}(t)}{dt^2}-\frac{dv_c(t)}{dt}\left(\delta(t-\sigma_{k-1})-\delta(t-\sigma_k)\right)\\&-\frac{d\left((v_c(t)(\delta(t-\sigma_{k-1})-\delta(t-\sigma_k))\right)}{dt}\\&=A_kv_{c,k}(t)\\&+B_k\left(\frac{dv_{c,k}(t)}{dt}-v_c(t)\left(\delta(t-\sigma_{k-1})-\delta(t-\sigma_k)\right)\right)\\&+C_kv_{i,k}(t)\end{aligned}\quad(76)$$

For the N-path filter (76) reduces to (18) after reintroducing the infinite summation.

REFERENCES

[1] H. Darabi, A. Mirzaei, and M. Mikhemar, "Highly integrated and tunable RF front ends for reconfigurable multiband transceivers: A tutorial," *IEEE Trans. Circuits Syst. I, Reg. Papers*, vol. 58, pp. 2038–2050, 2011.

[2] A. Ghaffari, E. A. M. Klumperink, and B. Nauta, "A differential 4-path highly linear widely tunable on-chip band-pass filter," in *Proc. 2010 IEEE Radio Freq. Integr. Circuits Symp. (RFIC)*, pp. 299–302.

[3] A. Mirzaie, A. Yazdi, Z. Zhou, E. Chang, P. Suri, and H. Darabi, "A 65 nm CMOS quad-band SAW-less receiver for GSM/GPRS/EDGE," in *Proc. 2010 IEEE Symp. VLSI Circuits (VLSIC)*, pp. 179–180.

[4] C. Andrews and A. C. Molnar, "Implications of passive mixer transparency for impedance matching and noise figure in passive mixer-first receivers," *IEEE Trans. Circuits Syst. I, Reg. Papers*, vol. 57, pp. 3092–3103, 2010.

[5] A. Ghaffari, E. A. M. Klumperink, M. C. M. Soer, and B. Nauta, "Tunable high-Q N-path band-pass filters: Modeling and verification," *IEEE J. Solid-State Circuits*, vol. 46, pp. 998–1010, 2011.

[6] A. Mirzaei, H. Darabi, and D. Murphy, "A low-power process-scalable super-heterodyne receiver with integrated high-Q filters," *IEEE J. Solid-State Circuits*, vol. 46, pp. 2920–2932, 2011.

[7] A. Ghaffari, E. Klumperink, and B. Nauta, "8-Path tunable RF notch filters for blocker suppression," in *2012 IEEE Int. Solid-State Circuits Conf. Dig. Tech. Papers (ISSCC)*, pp. 76–78.

[8] M. Darvishi, R. van der Zee, E. A. M. Klumperink, and B. Nauta, "Widely tunable 4th order switched Gm-C Band-pass filter based on N-path filters," *IEEE J. Solid-State Circuits*, vol. 47, pp. 3105–3119, 2012.

[9] M. Darvishi, R. van der Zee, E. Klumperink, and B. Nauta, "A 0.3-to-1.2GHz tunable 4th-order switched gm-C bandpass filter with 55 dB ultimate rejection and out-of-band IIP3 of +29 dBm," in *2012 IEEE Int. Solid-State Circuits Conf. Dig. Tech. Papers (ISSCC)*, pp. 358–360.

[10] A. Mirzaei, H. Darabi, and D. Murphy, "Architectural evolution of integrated m-phase high-Q bandpass filters," *IEEE Trans. Circuits Syst. I, Reg. Papers*, vol. 59, pp. 52–65, 2012.

[11] M. Darvishi, R. van der Zee, and B. Nauta, "Design of active N-path filters," *IEEE J. Solid-State Circuits*, vol. 48, pp. 2962–2976, 2013.

[12] Z. Lin, P. I. Mak, and R. P. Martins, "Analysis and modeling of a gain-boosted N-path switched-capacitor bandpass filter," *IEEE Trans. Circuits Syst. I, Reg. Papers*, vol. PP, pp. 1–9, 2014.

[13] A. Ghaffari, E. A. M. Klumperink, F. E. van Vliet, and B. Nauta, "Simultaneous spatial and frequency-domain filtering at the antenna inputs achieving up to +10 dBm out-of-band/beam P1dB," in *2013 IEEE Int. Solid-State Circuits Conf. Dig. Tech. Papers (ISSCC)*, pp. 84–85.

[14] A. Ghaffari, E. A. M. Klumperink, F. E. van Vliet, and B. Nauta, "A 4-Element Phased-Array System with Simultaneous Spatial- and Frequency-Domain Filtering at the Antenna Inputs," *IEEE J. Solid-State Circuits*, 2014, accepted for publication.

[15] L. E. Franks and I. W. Sandberg, "An alternative approach to the realization of network transfer functions: The N-path filter," *Bell Sys. Tech. J.*, vol. 39, pp. 1321–1350, 1960.
[16] L. Franks and F. Witt, "Solid-state sampled-data bandpass filters," in *1960 IEEE Int. Solid-State Circuits Conf. Dig. Tech. Papers*, pp. 70–71.
[17] A. Ghaffari, E. A. M. Klumperink, and B. Nauta, "Tunable n-path notch filters for blocker suppression: Modeling and verification," *IEEE J. Solid-State Circuits*, vol. 48, pp. 1370–1382, 2013.
[18] M. C. M. Soer, E. A. M. Klumperink, P. T. de Boer, F. E. van Vliet, and B. Nauta, "Unified frequency-domain analysis of switched-series-rc passive mixers and samplers," *IEEE Trans. Circuits Syst. I, Reg. Papers*, vol. 57, pp. 2618–2631, 2010.
[19] A. El Oualkadi, M. El Kaamouchi, J. M. Paillot, D. Vanhoenacker-Janvier, and D. Flandre, "Fully integrated high-Q switched capacitor bandpass filter with center frequency and bandwidth tuning," in *Proc. 2007 IEEE Radio Freq. Integr. Circuits (RFIC) Symp.*, pp. 681–684.
[20] C. Andrews, L. Changhyuk, and A. Molnar, "Effects of LO harmonics and overlap shunting on N-phase passive mixer based receivers," in *Proc. 2012 ESSCIRC (ESSCIRC)*, pp. 117–120.
[21] A. Mirzaei and H. Darabi, "Analysis of imperfections on performance of 4-phase passive-mixer-based high-Q bandpass filters in saw-less receivers," *IEEE Trans. Circuits Syst. I, Reg. Papers*, vol. 58, pp. 879–892, 2011.
[22] A. Molnar and C. Andrews, "Impedance, filtering and noise in n-phase passive CMOS mixers," in *Proc. 2012 IEEE Custom Integr. Circuits Conf. (CICC)*, pp. 1–8.
[23] T. Ström and S. Signell, "Analysis of periodically switched linear circuits," *IEEE Trans. Circuits Syst.*, vol. CAS-24, pp. 531–541, 1977.
[24] M. Tenenbaum and H. Pollard, *Ordinary Differential Equations*. New York: Dover, 1985.

Lammert Duipmans received his M.Sc. degree from the University of Twente, The Netherlands, in 2013. His M.Sc. thesis deals with the suppression of harmonic folding effects in N-path filters by pre-filtering, and the analysis in this paper is largely based on his thesis.

Remko E. Struiksma received his B.Eng. degree from NHL University of Applied Sciences, The Netherlands, in 2006, and his MSc degree from the University of Twente, The Netherlands, in 2011. After this, he joined the IC Design group of the University of Twente as research assistant. His research work focuses on reconfigurable receivers and N-path filters.

Eric A. M. Klumperink received his Ph.D. from the University of Twente, Enschede, The Netherlands in 1997, and is currently an Associate Professor there with research focus on radio frequency ICs and beamforming. He served as Associate Editor for IEEE TRANSACTIONS ON CIRCUITS AND SYSTEMS—PART I: REGULAR PAPERS, TRANSACTIONS ON CIRCUITS AND SYSTEMS—PART II: EXPRESS BRIEFS and the IEEE JOURNAL OF SOLID-STATE CIRCUITS, and is a TPC member of ISSCC and RFIC. He serves as IEEE Distinguished lecturer and is co-recipient of the 2002 and 2009 ISSCC Van Vessem Outstanding Paper Award.

Bram Nauta (F'08) received his Ph.D. degree from the University of Twente, Enschede, The Netherlands, in 1991. After 7 years in Philips Research labs, he returned as full professor, heading the IC Design group. He served as TPC member of the major conferences in the field, and was program chair of ISSCC and the Editor-in-Chief of the IEEE JOURNAL OF SOLID-STATE CIRCUITS. He is IEEE fellow, member of IEEE-SSCS AdCom and co-recipient of the 2002 and 2009 ISSCC Van Vessem Outstanding Paper Award.

Frank E. van Vliet received his Ph.D. degree from Delft University of Technology, The Netherlands. He joined TNO (Netherlands Organization for Applied Scientific Research) in 1997, where he is currently a Principal Scientist responsible for MMIC, antenna, and transmit & receive module research. Since 2007, he is also a Professor in microwave integration in the ICD group of the University of Twente, The Netherlands. He has (co-)authored well over 100 peer-reviewed publications.